JACS
JOURNAL OF THE AMERICAN CHEMICAL SOCIETY
Article
pubs.acs.org/JACS

Spanning Four Mechanistic Regions of Intramolecular Proton-Coupled Electron Transfer in a $Ru(bpy)_3^{2+}$–Tyrosine Complex

Tania Irebo,[†] Ming-Tian Zhang,[†] Todd F. Markle, Amy M. Scott,[‡] and Leif Hammarström*

Photochemistry and Molecular Science, Department of Chemistry, Ångström Laboratory, Uppsala University, Box 532, SE-751 20 Uppsala, Sweden

Supporting Information

ABSTRACT: Proton-coupled electron transfer (PCET) from tyrosine (TyrOH) to a covalently linked $[Ru(bpy)_3]^{2+}$ photosensitizer in aqueous media has been systematically reinvestigated by laser flash-quench kinetics as a model system for PCET in radical enzymes and in photochemical energy conversion. Previous kinetic studies on Ru–TyrOH molecules (Sjödin et al. J. Am. Chem. Soc. 2000, 122, 3932; Irebo et al. J. Am. Chem. Soc. 2007, 129, 15462) have established two mechanisms. Concerted electron–proton (CEP) transfer has been observed when pH < pK_a(TyrOH), which is pH-dependent but not first-order in $[OH^-]$ and not dependent on the buffer concentration when it is sufficiently low (less than ca. 5 mM). In addition, the pH-independent rate constant for electron transfer from tyrosine phenolate ($TyrO^-$) was reported at pH >10. Here we compare the PCET rates and kinetic isotope effects (k_H/k_D) of four Ru–TyrOH molecules with varying $Ru^{III/II}$ oxidant strengths over a pH range of 1–12.5. On the basis of these data, two additional mechanistic regimes were observed and identified through analysis of kinetic competition and kinetic isotope effects (KIE): (i) a mechanism dominating at low pH assigned to a stepwise electron-first PCET and (ii) a stepwise proton-first PCET with OH^- as proton acceptor that dominates around pH = 10. The effect of solution pH and electrochemical potential of the $Ru^{III/II}$ oxidant on the competition between the different mechanisms is discussed. The systems investigated may serve as models for the mechanistic diversity of PCET reactions in general with water (H_2O, OH^-) as primary proton acceptor.

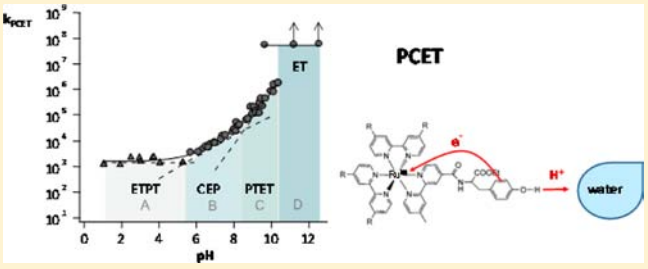

INTRODUCTION

Proton-coupled electron transfer (PCET) is an elementary reaction where both electrons and protons are transferred and is prevalent in radical enzymes,[1−3] biological energy conversion,[4−9] and in catalytic water splitting.[10−13] Recent attention has focused on gaining a detailed mechanistic understanding of PCET for solar fuel production by artificial photosynthesis,[10−13] where sunlight is captured and used to drive fuel forming reactions, as in eqs 1–3:

$$2H_2O \rightarrow O_2 + 4H^+ + 4e^- \quad (1)$$

$$2H^+ + 2e^- \rightarrow H_2 \quad (2)$$

$$CO_2 + 2H^+ + 2e^- \rightarrow HCOOH \quad (3)$$

PCET is an intimate part of the mechanistic steps of catalysis, where proton transfer may have a large impact on the energetics and rate of electron transfer, and vice versa.[14−19] The detailed studies and understanding of electron transfer has enabled the construction of efficient molecular solar cells.[20,21] A similarly detailed understanding of PCET is now necessary to design efficient systems for solar fuels production. PCET is fundamentally more complicated than electron transfer because two particles are being transferred, and there are a number of mechanistic pathways that must be considered. Therefore, it is important to have an understanding of the experimental markers of these various mechanisms and the conditions under which they are favored.

Model systems with phenol (PhOH) and tyrosine (TyrOH) derivatives have been the focus of several recent studies that examine the various parameters that influence PCET. Of particular interest has been PCET oxidation with water as proton acceptor,[13,15,22−33] which is encountered in both enzymes and water oxidation catalysts. The studies have led to interesting observations and discussions regarding the special character of water as acceptor in PCET reactions. The pK_a of PhOH decreases from 10 to −2 upon oxidation, and as a consequence, the redox potential is strongly dependent on protonation state: $E^\circ_{PhOH^{\bullet+}/PhOH}$ = 1.46 V vs NHE while $E^\circ_{PhO^\bullet/PhO^-}$ = 0.72 V.[34,35] This provides for strong energetic electron–proton coupling, as illustrated in Pourbaix diagrams (Figure 1). Of paramount interest for PCET is the mechanisms that this may lead to: PCET may occur by stepwise mechanisms, with either the proton or electron transfer as the first step (PTET or ETPT, respectively), or in a single, concerted electron–proton tunneling step (CEP). CEP is often energetically favored, as it utilizes all reaction free energy in a

Received: June 13, 2012
Published: August 21, 2012

   dx.doi.org/10.1021/ja3053859 | J. Am. Chem. Soc. 2012, 134, 16247–16254

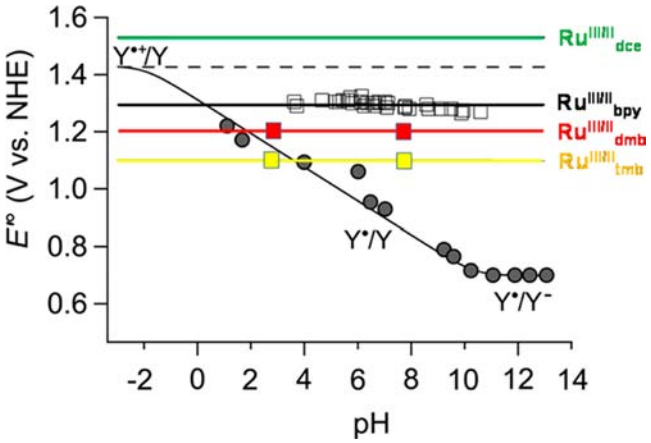

Figure 1. The apparent standard potential for the $Ru^{III/II}$ couple in the corresponding Ru–alanine reference complexes (squares) and that for tyrosine oxidation (dots) replotted from ref 34. The lines for the $Ru^{III/II}$ and $TyrO^{\bullet}/TyrO^{-}$ ($Y^{\bullet}/Y^{-}$) data are linear, pH-independent fits, and the line for $TyrO^{\bullet}/TyrOH$ ($Y^{\bullet}/Y$) is a linear fit with a slope of −59 mV/pH. The dashed red line indicates the pH-independent $TyrO^{\bullet}H^{+}/TyrOH$ ($Y^{\bullet+}/Y$) potential. The potentials for Ru_{dmb} (red) and Ru_{tmp} (yellow) are measured in this study (see the text) while the data for Ru_{bpy} (black) and Ru_{dce} (green) are taken from ref 22.

single step, but is more complex because of the simultaneous tunneling of the electron and proton.

The rate of phenol oxidation in aqueous solution typically depends on pH due to the pH-dependent concentration of the more easily oxidized and much more reactive phenolate form (PhO^{-}) of tyrosine

$$k_{PCET} = k_{PhOH} f_{PhOH} + k_{PhO^-} f_{PhO^-} \quad (4)$$

where f_{PhOH} and f_{PhO^-} are the pH-dependent fractions of phenol and phenolate, respectively. However, previously in our lab Sjödin et al.[22] reported that the rate of intramolecular PCET in a $Ru^{III}(bpy)_3$–tyrosine complex (**Ru_{bpy}–Y**; Figure 2) showed a pH-dependence also of the phenol form, i.e., that k_{PhOH} was pH-dependent, which was attributed to a CEP reaction. In that data $\log(k_{PhOH})$ was found to increase by 0.5 per pH unit, which is much weaker than the first-order dependence on $[OH^{-}]$ expected for reaction via the phenolate form ($k_{PhO^-} f_{PhO^-}$). The results cannot be explained by the various buffers used or by simple bimolecular reactions with OH^{-}. Extensive studies using different buffers and buffer concentrations (0–0.5 M) showed that the PCET rate was unaffected by buffer concentrations below ca. 5 mM.[24] These reports have led to much debate, as PCET from phenol with water as proton acceptor is not expected to be pH-dependent.[13,26,36]

Here we report a mechanistic study of intramolecular PCET in a series of covalently linked Ru^{III}–tyrosine complexes (Figure 2) by direct kinetic measurements using a laser flash-quench method.[22−24,37] The rapid, intramolecular reaction and the relatively slow $TyrOH–TyrO^{-}$ equilibrium allows us to study the pH-dependence of k_{PCET} without interference from the fraction of $Ru^{III}–TyrO^{-}$ species ($k_{PhO^-} f_{PhO^-}$ in eq 4). Our data suggests that we can observe up to four different mechanistic regimes for tyrosine oxidation in a single Ru–TyrOH complex with water as proton acceptor, depending on the solution pH: ETPT, CEP, PTET in Ru–TyrOH, and ET in $Ru–TyrO^{-}$. The PCET mechanisms are kinetically distinct and k_{PhOH} in eq 4 is given by a sum of three terms, $k_{PhOH} = k_{ETPT} + k_{CEP} + k_{PTET}$, each with a different pH-dependence and kinetic isotope effect (KIE). By tuning pH and the oxidant strength of the Ru^{III} species, the different mechanisms can be enhanced or suppressed. This gives a direct experimental manifestation of the mechanistic complexity of PCET in water and may serve as an experimental basis for further studies and understanding of this fundamental class of reactions.

RESULTS AND DISCUSSION

In the present study, we reinvestigated the PCET reactions of **Ru_{bpy}–Y** in a larger pH range than previously reported,[24] spanning nearly 12 units. We also present results for two new complexes, **Ru_{dmb}–Y** and **Ru_{tmb}–Y**, for which the Ru^{III} is a somewhat weaker oxidant. This allows us to specifically examine three aspects: (1) In analogous complexes with a stronger oxidant (**Ru_{dce}–Y**), a pH-independent region was observed at pH < 8 and was assigned to a stepwise ETPT mechanism.[23] Could a pH-independent ETPT reaction be observed also in **Ru_{bpy}–Y** if the pH value is low enough? (2) For **Ru_{bpy}–Y**, PTET with OH^{-} as the acceptor should be PT-limited and near diffusion-controlled (see below). This would lead to a first-order dependence on $[OH^{-}]$ and may have been on the limit of being resolved in the previous studies. Could we find evidence for this mechanism by obtaining a more extensive data set around pH = 10? (3) Can we tune the preference between these mechanisms and the CEP mechanism previously observed around neutral pH for **Ru_{bpy}–Y** by using Ru complexes with different $Ru^{III/II}$ potentials?

A key point we emphasize is that studies of bimolecular oxidation are complicated by the strong pH-dependence of k_{obs} due to the $k_{PhO^-} f_{PhO^-}$ term (eq 4), and the observed reactions are also convoluted with diffusion steps. However, in **Ru_{bpy}–Y** intramolecular PCET can be followed directly by laser-induced transient absorption spectroscopy at sufficiently low concentrations such that bimolecular reactions can be neglected. Moreover, as long as moderate buffer concentrations are used, the TyrOH/$TyrO^{-}$ equilibrium reaction is much slower than electron transfer in the deprotonated species $Ru^{III}–TyrO^{-}$ (see

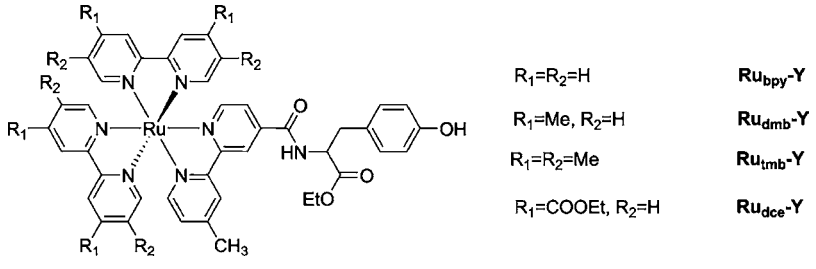

Figure 2. Structures of the complexes studied in this paper and of **Ru_{dce}–Y** from ref 22.

dx.doi.org/10.1021/ja3053859 | J. Am. Chem. Soc. 2012, 134, 16247–16254

below). The fractions of Ru^{III}−TyrOH and Ru^{III}−$TyrO^-$ present before the laser flash therefore react and can be studied separately in the same experiment, giving biexponential kinetics around pH = pK_a. Thus, the pH-dependence of the Ru^{III}−TyrOH reaction can be followed over a large pH interval without interference from the fraction of $TyrO^-$ present (cf. eq 4 for a bimolecular reaction). The intramolecular reaction is free of diffusion steps between the Ru^{III} and TyrOH/$TyrO^-$ reactants, and the reaction can be followed on the nanosecond−microsecond time scale. On this time scale TyrOH undergoes only single-electron oxidation/PCET without complications from further oxidation or $TyrO^•$ dimerization. Only ca. 1 μM reactants are converted in each flash so that local pH variations are negligible when using >10^{-5} M buffers. These advantages make laser flash−quench studies of sensitizer−TyrOH complexes highly useful for detailed examination of the pH-dependent PCET kinetics.

The electrochemical data for the complexes are shown in Figure 1. The $Ru^{III/II}$ potential of the Ru unit in $\mathbf{Ru_{bpy}}$−**Y**, $E^{\circ\prime}_{Ru(III/II)}$ = 1.29 V vs NHE, is pH-independent,[23] as is also the case for $[Ru(bpy)_3]^{2+}$.[23,39] It is thus reasonable to assume that this holds also for the other $Ru^{III/II}$ couples. For $\mathbf{Ru_{dmb}}$−**Y** and $\mathbf{Ru_{tmb}}$−**Y**, $E^{\circ\prime}_{Ru(III/II)}$ was determined from cyclic and differential pulse voltammetry (Supporting Information, Figure S5) to be 1.20 and 1.15 V vs NHE, respectively, and the values at pH ≈ 3 and ≈8 were indeed indistinguishable (Figure 1). For $\mathbf{Ru_{dce}}$−**Y** the value of $E^{\circ\prime}_{Ru(III/II)}$ = 1.53 V vs NHE was used.[23] The tyrosine data in Figure 1 is in close agreement to that determined for $\mathbf{Ru_{bpy}}$−**Y**,[23] with $E^{\circ\prime}_{TyrO^•/TyrO^-}$ = 0.70 V at high pH, and a Nernstian dependence of $E^{\circ\prime}_{TyrO^•/TyrOH}$ below the pK_a value of 10.3.

The PCET reaction (eq 6) was initiated by photo-oxidizing the Ru unit with a 10 ns laser flash at 460 nm in the presence of methyl viologen (MV^{2+}), $[Co(NH_3)_5Cl]^{2+}$, or in one case (Figure 4) $[Ru(NH_3)_6]^{3+}$, as external acceptor (eq 5).[22−24]

$$*Ru^{II}\text{−TyrOH} + A \rightarrow Ru^{III}\text{−TyrOH} + A^- \quad (5)$$

$$Ru^{III}\text{−TyrOH} \rightarrow Ru^{II}\text{−}TyrO^• + H^+ \quad (6)$$

The quenching reactions (eq 5) are much faster than PCET (eq 6) and do not interfere kinetically. The PCET reaction 6 was monitored, mainly by the transient absorption changes at 450 nm (Ru^{II} bleach) and 410 nm ($TyrO^•$ absorption). Examples of transient absorption data are given in Figures 3 and 4 and in Figure S1 of the Supporting Information. With MV^{2+} as acceptor, the recombination reaction 7 occurred on longer time scales, regenerating the tyrosine, which was followed at 600 nm ($MV^{•+}$ maximum).

$$Ru^{II}\text{−}TyrO^• + MV^{•+} + H^+ \rightarrow Ru^{II}\text{−TyrOH} + MV^{2+} \quad (7)$$

For the slowest PCET reactions the irreversible acceptor $[Co(NH_3)_5Cl]^{2+}$ was used instead to avoid excessive recombination between Ru^{III} and $MV^{•+}$ (see Experimental Section).

Kinetic Data. Figure 5 shows the observed PCET rate constants (eq 6) as a function of pH for the three complexes. The bimolecular reactions between Ru−TyrOH complexes are insignificant compared to the intramolecular PCET, as described above.[40] Starting with $\mathbf{Ru_{bpy}}$−**Y**, the data show rapid electron transfer in the Ru−$TyrO^-$ fraction that is the dominating species at pH > 10 (Figure 5a, region D):

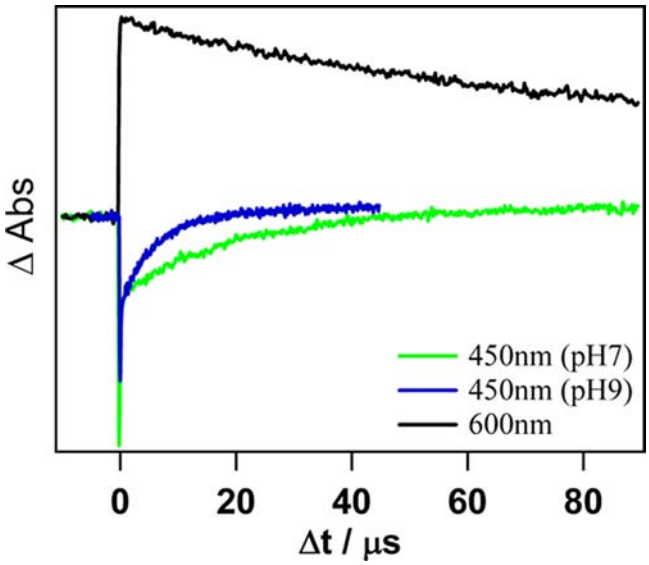

Figure 3. Transient absorption kinetic traces for a sample with $\mathbf{Ru_{bpy}}$−**Y** and MV^{2+} collected at 450 nm (Ru^{II} bleach: green line, pH = 7.5; blue line, pH = 9) and 600 nm (MV^+ absorption: black line). The initial "spike" in the 450 nm signal is due to the quenching reaction (eq 5) and is followed by the pH-dependent PCET reaction (eq 6). The 600 nm signal eventually decays via recombination (eq 7).

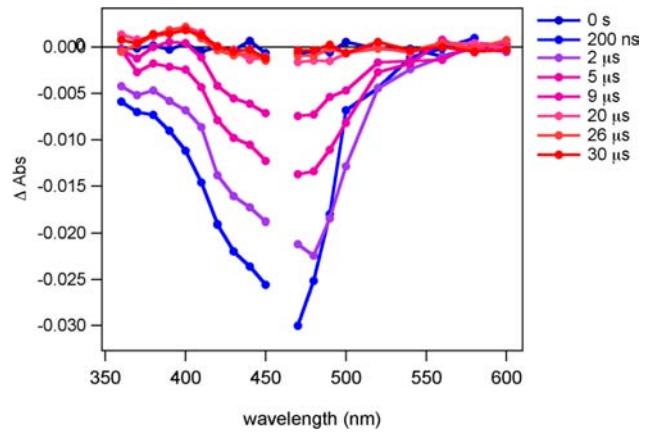

Figure 4. Transient absorption spectra of $\mathbf{Ru_{bpy}}$−**Y** at pH = 9.1. $[Ru(NH_3)_6]^{3+}$ is used as quenching electron acceptor. During the PCET reaction 6 the Ru^{II} bleach recovers and the $TyrO^•$ absorption at 410 increases.

$$Ru^{III}\text{−}TyrO^- \rightarrow Ru^{II}\text{−}TyrO^• \quad (8)$$

The rate of reaction 8 was close to or faster than the time resolution of the experiment (ca. 10 ns), so the rate constant data in region D of Figure 5a represent lower limits. At pH < pK_a, instead the Ru^{III}−TyrOH fraction (eq 6) dominates the signal and shows a smaller and pH-dependent rate constant. Around pH = pK_a the reaction is biphasic, because the fractions of Ru^{III}−TyrOH and Ru^{III}−$TyrO^-$ at equilibrium before the laser flash are both significant, as was reported before.[22−24]

At the lower pH range studied here, it becomes obvious that the PCET rate constant levels out to a pH-independent value of ca. 1.4 × 10^3 s^{-1} (region A in Figure 5a). Note that this cannot be explained by the use of different acceptors, as identical rates of PCET in $\mathbf{Ru_{bpy}}$−**Y** were observed with MV^{2+} and $[Co(NH_3)_5Cl]^{2+}$ at pH values where both could be used. Also, the use of $[Co(NH_3)_5Cl]^{2+}$ did not significantly affect pH

dx.doi.org/10.1021/ja3053859 | J. Am. Chem. Soc. 2012, 134, 16247−16254

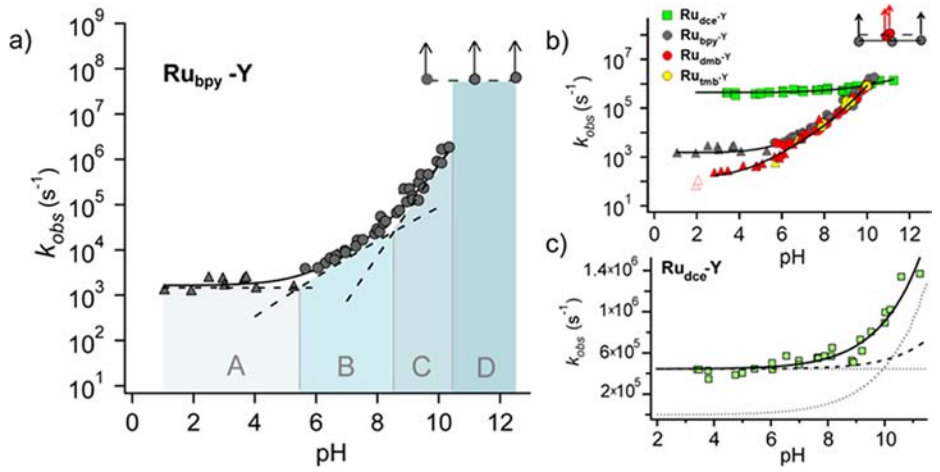

Figure 5. The rate constant for intramolecular TyrOH/TyrO$^-$ oxidation as a function of pH, in the complexes of Figure 2 (standard deviation typically <2% in regions B and C and 5−10% in region A; see Table S1, Supporting Information). Triangles indicate data obtained with $[Co(NH_3)_5Cl]^{2+}$ instead of methyl viologen as electron acceptor in the laser flash-quench experiments. (a) Data and mechanistic regimes for **Ru$_{bpy}$−Y**. The solid line is a fit using eq 9, the dashed lines indicate the three term contributions (regions A−C), the dashed line in region D is a linear fit to the data. (b) Comparison of the data for all complexes. (c) The data for **Ru$_{dce}$−Y** on a linear scale. The dotted lines are the contributions of the first two terms of eq 9 (no contribution from the third term is seen). The dashed line shows what the sum of the two first terms would have been if the value of k_2 had been equal to that for Ru$_{bpy}$−Y. Conditions: see Experimental Section.

(see Experimental Section) and the same rate constants were also obtained at pH = 1−4 using a 10-fold higher buffer concentration. Thus, we conclude that the rate of PCET becomes pH-independent at pH < 5.

Lastly, by taking more data points than before in the region around pH = 10, at a buffer concentration of 0.5 mM, which is clearly below the buffer-dependent region[24] (see Supporting Information), we observe also here a different pH-dependence (region C in Figure 5a). The slope is clearly steeper than around pH = 7 (region B) and agrees with a first-order dependence on [OH$^-$] (slope = 1). Thus, it appears there are three different regimes of PCET oxidation for the Ru−TyrOH form (in addition to electron transfer in the Ru−TyrO$^-$ form): one pH-independent regime that dominates at low pH values (A), one with a slope = 1 that dominates at high pH (C), and one with an intermediate slope ≈ 0.5 (B). Only the latter reaction was reported before for **Ru$_{bpy}$−Y**.[22−24] Figure 5a shows a fit of a sum of three terms to the PCET data, according to eq 9:

$$k_{PCET} = k_1 + k_2 \times 10^{0.5pH} + k_3 \times 10^{pH} \quad (9a)$$

The last term was identified as a PTET reaction that is first-order in [OH$^-$] (see below) so that

$$k_3 \times 10^{pH} = k_{PTET}[OH^-] \quad (9b)$$

where, obviously, $k_{PTET} = k_3 \times 10^{14}$ M^{-1}. For the second term, the mechanism behind its pH-dependence is not clear (e.g., half-order in [OH$^-$], inverse half-order in [H$^+$], or more complex), so we refrain from making a similar assignment as in eq 9b. In the logarithmic plot the terms are shown as three straight, dashed lines, with slopes of 0, 0.5 and 1, representing the dominating mechanism in region A, B, and C, respectively. For **Ru$_{bpy}$−Y** the values obtained are $k_1 = 1.4 \times 10^3$ s^{-1}; $k_2 = 2.3$ s^{-1} (i.e., $k_2 \times 10^{0.5pH} = 7 \times 10^3$ at pH = 7) and $k_3 = 7.3 \times 10^{-5}$ s^{-1} (i.e., $k_{PTET} = 7.3 \times 10^9$ M^{-1} s^{-1}). Note that a fit using only the first and last terms gives very poor agreement with the data in the region of pH = 5−9 (Figure 6). The kinetic isotope effect (KIE = k_H/k_D) was measured by replacing water with D_2O and

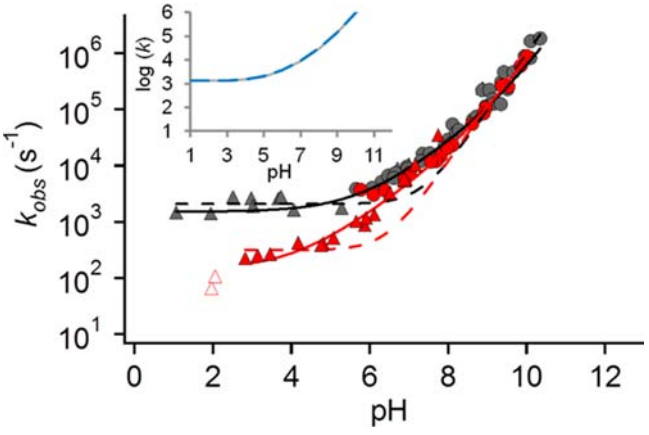

Figure 6. pH-dependent data for **Ru$_{bpy}$−Y** (gray) and **Ru$_{dmb}$−Y** (red) with three-term fits according to eq 9 (solid lines) as in Figure 5. The dashed lines show fits using only two terms: $k_1 + k_3 \times 10^{pH}$. Inset: the fit for **Ru$_{bpy}$−Y** is compared without (gray solid line) and with (blue dashed line) an additional term from the kinetic effect of 0.5 mM phosphate buffer (see the text); the latter apparently gives a negligible contribution to the observed rate constant.

varies significantly between the three regions (Table 1). Further support for the three different regimes comes from a comparison of the kinetic data with data for the other Ru−TyrOH complexes and from comparison with diffusion limited

Table 1. Kinetic Isotope Effects on k_{PCET} at 298 K and Activation Energies

	Ru$_{dmb}$−Y		**Ru$_{bpy}$−Y**		**Ru$_{dce}$−Y^d**	
region	k_H/k_D	E_a (eV)	k_H/k_D[c]	E_a (eV)	k_H/k_D	E_a (eV)
A	–	–	2.0(±0.3)[a]	0.44[a]	2[d]	0.26[d]
B	5.3(±1.0)[b]	–	3.0(±0.8)[b]	0.46[b]	>10[d]	0.60[d]
C	8.2(±2.3)[c]	–	5.6(±0.6)[c]	0.38[c]	–	–

[a]At pH = 2−3. [b]At pH = 6.9. [c]At pH = 9.7. [d]From ref 23

dx.doi.org/10.1021/ja3053859 | J. Am. Chem. Soc. 2012, 134, 16247−16254

rates for deprotonation of tyrosine by OH^-, as discussed in the following paragraphs.

Note that under the conditions used here the rates are independent of the type and concentration of buffer used, as shown in ref 24 and discussed in the Supporting Information (Figures S2 and S3). We have measured the second-order rate constant for buffer-dependent PCET, where the base form of the buffer is the primary proton acceptor, using high buffer concentrations. At 0.5 mM of HPO_4^{2-} or borate,[24] these pseudo-first-order rate constant contributions saturate at 1.5×10^3 and ca. 5×10^3 s^{-1}, respectively, at pH > pK_a of the buffer (7.2 and 9.2, respectively) and decrease rapidly at lower pH values. This is much lower than the observed rate constants, so these contributions can be neglected [see Figures 6 (inset) and S3 (Supporting Information)]. In the absence of buffer, there is a relatively large uncertainty in pH at around neutral pH.[24] Therefore, a low buffer concentration was used in this study.

In $\mathbf{Ru_{dmb}}$–**Y** the Ru^{III} unit is a ca. 0.09 V weaker oxidant than in $\mathbf{Ru_{bpy}}$–**Y** (Figure 1). The data for $\mathbf{Ru_{dmb}}$–**Y** in Figure 5b show large qualitative similarities to that for $\mathbf{Ru_{bpy}}$–**Y**. Also here the fractions of Ru–TyrOH and Ru–$TyrO^-$ present before the laser flash react independently, giving biexponential kinetics around pH = 10. The rate of PCET is very similar to that for $\mathbf{Ru_{bpy}}$–**Y** at pH = 6–11, but continues to decrease at lower pH values and does not become clearly pH-independent in the range examined. A fit according to eq 9 gave $k_1 = 1.4 \times 10^2$ s^{-1}, $k_2 = 1.4$ s^{-1} (i.e., $k_2 \times 10^{0.5pH} = 4 \times 10^3$ at pH = 7), and $k_3 = 7 \times 10^{-5}$ s^{-1} (i.e., $k_{PTET} = 7 \times 10^9$ M^{-1} s^{-1}) (see Figure 5b). The last two terms are not significantly different from those in $\mathbf{Ru_{bpy}}$–**Y**, but the first term is 10-fold smaller. Therefore, the two-term fit in Figure 6 (dashed line of main figure) shows even worse agreement than for $\mathbf{Ru_{bpy}}$–**Y**. The data points around pH = 2 were excluded from the fit because $\Delta G^0 \approx 0$, and the observed rate constant may therefore not be limited by PCET but by irreversible dimerization of tyrosine radicals following pre-equilibrium PCET.

$\mathbf{Ru_{tmb}}$–**Y** was prepared and studied with focus on the pH-dependent regions at pH 6–10. Although the $Ru^{III/II}$ potential is 0.05 V lower than for $\mathbf{Ru_{dmb}}$–**Y**, the rates are not significantly different in this region (Figure 5b, yellow data points).

The Ru^{III} oxidant in $\mathbf{Ru_{dce}}$–**Y** is instead ca. 0.24 V stronger than in $\mathbf{Ru_{bpy}}$–**Y**; the kinetic data is taken from ref 23. The Ru–$TyrO^-$ reaction was too rapid to be measured. The PCET rate of the Ru–TyrOH form is pH-independent in a large pH interval but increases with pH at higher pH values. This is seen more clearly on a linear scale (Figure 5c) and was assigned to an ETPT reaction at low pH and a CEP reaction dominating at high pH. The solid line is a fit to the data using a sum of a constant term ($k_1 \approx 4 \times 10^5$ s^{-1}) and an exponential increase (k_2), and the dotted lines indicate the term contributions. The exponential term (k_2) corresponds to a straight line in the logarithmic plot of Figure 5b with the same slope = 0.5 as for $\mathbf{Ru_{bpy}}$–**Y** at neutral pH.

PCET Mechanisms. To gain a thorough understanding of the parameters that influence the PCET mechanisms, a comparison of the different Ru–TyrOH complexes, their pH-dependent kinetics, and KIE are used to assign the dominating mechanisms for the different pH regions observed.

ET from $TyrO^-$ (region D). Beginning with what is the simplest case, the predominant reaction at pH > pK_a is the Ru^{III}–$TyrO^-$ species that reacts by pure electron transfer (ET; eq 6). Note that the equilibrium reaction TyrOH ↔ $TyrO^-$ (k_{PT1}, k_{-PT1} and k'_{PT1}, k'_{-PT1} in Scheme 1) is slow compared to the observed intramolecular ET reaction (k_{ET2}); see footnotes 41 and 42. Therefore, the Ru^{III}–$TyrO^-$ and Ru^{III}–TyrOH species created by each laser excitation react separately without interconversion, giving rise to biexponential kinetics around pH = 10 (pK_a of TyrOH). This is very different from bimolecular reactions where the $TyrO^-$ and TyrOH fractions react with the same oxidants, giving rise to single exponential kinetics according to eq 4.

Scheme 1. Mechanisms of PCET with Water (top) or OH^- (bottom) as Primary Proton Acceptor[a]

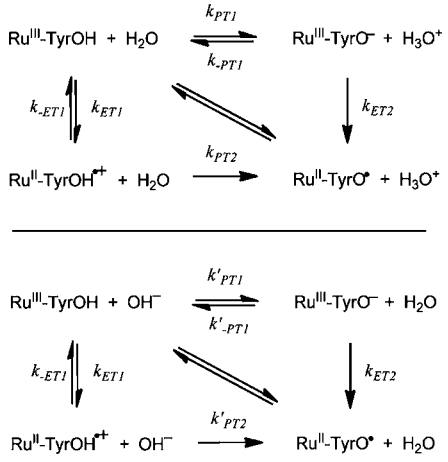

[a]The stepwise pathways ETPT and PTET follow consecutive horizontal and vertical arrows, while the concerted CEP reaction is indicated by the diagonal arrows.

PTET from TyrOH (region C). Scheme 1 shows the different mechanisms for PCET from TyrOH that must be considered for oxidations below pH ≈ 10. TyrOH deprotonation is faster by OH^- than by water, giving an expected value of $k'_{PT} \approx 1 \times 10^{10}$ M^{-1} s^{-1}. The rate constant for $\mathbf{Ru_{bpy}}$–**Y** and $\mathbf{Ru_{dmb}}$–**Y** around pH = 9–11 (the last term of eq 9) has the expected first-order dependence on [OH^-], and the fit gives rate constants of $k_{PTET} = 7.3 \times 10^9$ M^{-1} s^{-1} and $k_{PTET} = 7 \times 10^9$ M^{-1} s^{-1}, respectively, for the two complexes, in good agreement with the expected value for a diffusion-controlled reaction with OH^-. The rate constant is the same for both compounds, in spite of their difference in $E^0_{Ru(III/II)}$ values, which argues against a CEP mechanism with OH^- as acceptor. Furthermore, in the Ru–TyrOH – OH^- encounter complex, the downhill PT should be barrierless and occur with $k_{PT} \approx 6 \times 10^{12}$ s^{-1}.[41] In contrast, CEP is strongly nonadiabatic, as the electron transfer is mediated via several saturated bonds and should not be able to compete on this time scale. On the basis of these observations, we can assign the dominating PCET mechanism in this region to PT-limited PTET, with OH^- as primary proton acceptor. For $\mathbf{Ru_{dce}}$–**Y** of ref 22, the other mechanisms are relatively rapid and the diffusion-controlled reaction with [OH^-] would only have been apparent in the single data point at pH ≈ 11. Here the fraction of TyrOH is small (≈0.1) and the signal amplitude correspondingly small. Therefore, we cannot exclude that the PTET reaction was overlooked in ref 22.

The apparent kinetic isotope effect observed for k_{PCET} (eq 9) can be explained by the lower autoprotolysis constant of D_2O: $K_w(H_2O) = 7.5K_w(D_2O)$.[43] As we compare H_2O and D_2O solutions with pH = pD, [OH^-] = 7.5[OD^-]. Thus, the pseudo-first-order rate constant k_3 would be expected to show a

dx.doi.org/10.1021/ja3053859 | J. Am. Chem. Soc. 2012, 134, 16247–16254

KIE = 7.5, which is in fair agreement with the observed values (in the PTET region, an error in pH of 0.1 corresponds to an error in KIE of ca. 25%). Consequently, $k_H/k_D \approx 1$ for the PTET reaction when compared at $[OH^-] = [OD^-]$, as can be expected for a diffusion-controlled reaction.

It is important to emphasize that this intramolecular PTET reaction of $Ru^{III}-TyrO^-$ is different from the typically observed bimolecular reaction with the small but reactive fraction of $TyrO^-$ that dominates in bimolecular reactions (eq 4). Thanks to the intramolecular nature of the present oxidation, we can assign this to a PTET reaction from TyrOH with OH^- as the proton acceptor.

CEP from TyrOH (region B). For PCET in the region pH ≈ 5.5−8.5 (Figure 5a) the dominating mechanism is represented by the middle term of eq 9, with $k_{PCET} \propto 10^{0.5pH}$. The CEP mechanism is implied here by ruling out the stepwise pathways. PTET would be too slow at these pH values to explain the observed rates; for example, at pH = 7 the value of $k'_{PT1}[OH^-] \approx 7 \times 10^2\ s^{-1}$, more than 10-fold lower than the observed rate constant (cf. above). ETPT, on the other hand, should be ET-limited as deprotonation of the tyrosine radical ($pK_a = -2$) is very fast, $k_{PT2} \approx 1 \times 10^{13}\ s^{-1}$.[44] Therefore, ETPT is expected to be rather insensitive to pH and hydrogen isotope, as discussed in the next section. In contrast, for **Ru_{bpy}−Y** and **Ru_{dmb}−Y** in region B, we found a pH-dependent rate and a significant value of KIE = 3−5 (Table 1). Thus, the PCET mechanism around neutral pH for **Ru_{bpy}−Y** and **Ru_{dmb}−Y** is assigned to a concerted PCET reaction (CEP), as reported before for **Ru_{bpy}−Y**.[22,24] We note that if the term $k_2 \times 10^{0.5pH}$ would be interpreted as a half-order dependence on $[OH^-]$, the concentration ratio $[OH^-]/[OD^-] = 7.5^{1/2} \approx 2.7$, which is somewhat too low to itself explain the KIE values. **Ru_{dmb}−Y** shows the same modest pH-dependent reaction as **Ru_{bpy}−Y**, but in this case it dominates down to at least pH = 2 and the pH-independent region A is not clearly reached. In sharp contrast, **Ru_{dce}−Y** has a high-potential $Ru^{III/II}$ couple and shows pH-independent rates up to pH = 8 and a pH-dependence only under the most basic conditions.[23]

The reason for the unusual pH-dependence displayed by this mechanism ($k_{CEP} \propto 10^{0.5pH}$) remains to be explained. However, control experiments show that the rate is independent of buffer at these concentrations (see Supporting Information). Also, simple first-order reactions with OH^- are too slow to explain the data (see above). Moreover, the $Ru^{III/II}$ potential (Figure 1) and the electronic coupling (H_{AB}^2, eq 10) via the amide link are also pH-independent. The latter is shown by the pH-independent rates over a large pH range for pure ET in Ru−tryptophan complexes using the same Ru complex[23,45] and for PCET in Ru−tyrosine complexes where an internal base is the primary proton acceptor.[46,47]

Sjödin et al.[22,23] suggested that the pH-dependent rate followed a Marcus-type dependence[48] on the overall free energy (ΔG^0, eq 10), as defined by the apparent standard potentials in Figure 1. They did note, however, that the pH-dependent TyrOH potential is due to proton dilution (mixing entropy) and that the driving force for the elementary CEP step with one or a few water molecules as proton acceptor should therefore not depend on pH. This problem has been emphasized by others.[13,26,36] The experimental result points toward a more complex microscopic description of the CEP reaction, which calls for further theoretical work. In the present study, we make the important observation that the rate of CEP in region B is not significantly different between **Ru_{bpy}−Y**, **Ru_{dmb}−Y**, and **Ru_{tmb}−Y**, in spite of a 0.14 V difference in $Ru^{III/II}$ potential. For **Ru_{dce}−Y** the rate is only about 2-fold higher, in spite of a 0.27 V higher potential than in **Ru_{bpy}−Y**. This shows that a dependence of k_{CEP} on driving force as in eq 10 does not hold up in these cases. This is indeed surprising, even disregarding the disputed pH-dependence in region B. At a given pH both ETPT and CEP reactions should depend on oxidant strength (which is an enthalpic difference) according to eq 10, and PT-limited reactions appear to be too slow for the observed rates.

Furthermore, a very similar pH-dependence as that shown in region B has been reported for Ru^{III}−tryptophan complexes, as well as for bimolecular oxidation of a tryptophan derivative with either $[Ru(bpy)_3]^{3+}$ or $[Ru(dmb)_3]^{3+}$, and assigned to a CEP reaction.[45,49] In the bimolecular studies the reaction was much faster with the stronger Ru^{III} oxidant,[49] in contrast to the present results. Moreover, when the tryptophan $Trp^{\bullet}H^+/TrpH$ potential of the Ru-linked system was increased using a bromide derivative, the observed k_{CEP} did decrease,[45] in clear contrast to the present results. As the $Trp^{\bullet}H^+$ pK_a decreased by bromination, the lower rates cannot be explained by PT-limited mechanisms. The very different results of driving force variations on the rate of CEP in Ru−TyrOH and Ru−TrpH complexes underscore our presently incomplete understanding of the important CEP reaction in water. Nevertheless, our results show that the rate of the CEP mechanism (region B) of the present series of Ru−TyrOH complexes appears to be nearly independent of driving force in the range of values examined.

$$k = \frac{2\pi}{\hbar} H_{AB}{}^2 \frac{1}{\sqrt{4\pi\lambda k_b T}} \exp\left(-\frac{(\Delta G^0 + \lambda)^2}{4\lambda k_b T}\right) \quad (10)$$

ETPT from TyrOH (region A). For **Ru_{dce}−Y**, which was reported previously, PCET is pH-independent at pH < 8 and showed a relatively small KIE, which was assigned to an ET-limited ETPT mechanism.[23] The assignment was supported by the direct spectroscopic observation of ETPT in an analogous Ru−tryptophan complex for which the energetics and pH-dependence was very similar. In **Ru_{dce}−Y** the rate-limiting initial ET step is even slightly exergonic, $\Delta G^\circ_{ET} = -0.07$ eV, as compared to $\Delta G^\circ_{ET} = +0.20$ eV for the corresponding reaction step in **Ru_{bpy}−Y**. The use of a stronger oxidant gives ETPT a better chance to compete with CEP.[23,45] We reasoned therefore that a similar switch to an ETPT mechanism might be observed in **Ru_{bpy}−Y** if the pH range was extended to lower values than examined before. In this study we indeed observe a pH-independent region for **Ru_{bpy}−Y** as well, at pH < 5. For **Ru_{dmb}−Y**, with an even weaker oxidant, no pH-independent region is reached, even at the lowest pH values employed. For **Ru_{bpy}−Y** at low pH, KIE = 2.0, which is identical to the value for **Ru_{dce}−Y** and smaller than for the CEP reactions in region B. Note that a small isotope effect for the pure ET reaction may be explained by the fact that not only the phenolic proton but the entire solvent is changed. This may affect accepting vibrational modes and solvent−solute coupling. There are several literature examples of pure electron transfer reactions for which the solvent KIE = 1.5−2.0.[50]

The relative rates for the ETPT reaction of **Ru_{bpy}−Y** and **Ru_{dce}−Y** correlate well with the predicted free-energy dependence of eq 10,[48] using an average value of $\lambda = 1.2$ eV as determined from the experimental activation energies for the two complexes. The predicted ratio k_{ETPT} for the two

complexes is 500, while the experimental value is 300, giving further support to our mechanistic assignment. Equation 10 also predicts that $k_{ETPT} \approx 1 \times 10^2$ s^{-1} in **Ru$_{dmb}$–Y**, where ΔG°_{ET} = +0.29 eV. This rationalizes the absence of a clear ETPT region in the experimental data for **Ru$_{dmb}$–Y**.

To conclude, we have assigned the pH-independent PCET reaction observed at low pH to an ETPT mechanism, rate-limited by the initial ET step. We cannot rule out a pH-independent CEP mechanism, however, but that would still be a mechanism distinct from that in region B. It would require an explanation for the existence of two different CEP mechanisms in regions A and B, respectively, with different pH-dependences and kinetic isotope effects, none of which is dependent on buffer or is simple first-order in [OH$^-$].

CONCLUDING REMARKS

We have found that TyrOH oxidation in the series of Ru^{III}–TyrOH complexes with water (H_2O and OH^-) as proton acceptor follows four separate mechanisms that dominate in different pH regions (A–D in Figure 5a) and are independent of buffer. First, in the fraction of Ru^{III}–TyrO$^-$ that dominates at pH > 10, the reaction is a pure ET. Second, for the Ru^{III}–TyrOH form of **Ru$_{bpy}$–Y** we found three different mechanisms: PT-limited PTET with OH^- as proton acceptor around pH = 10, CEP around pH = 7 with water as proton acceptor, and finally ET-limited ETPT (or possibly pH-independent CEP) at pH < 4. It is clear that the ETPT and PTET terms of eq 9 (k_1 and $k_3 \times 10^{pH}$) are not sufficient to describe the variation in rate with pH shown in Figure 5 (cf. Figure 6). The KIE at neutral pH where the CEP mechanism dominates is different from the KIEs for both ETPT and PTET. Moreover, while **Ru$_{bpy}$–Y** displays all mechanisms in the pH range examined, **Ru$_{dmb}$–Y** with a weaker oxidant does not show the ETPT region. These observations support the assignment to three distinct mechanisms at pH < 10 with distinct kinetic characteristics, rather than a single mechanism with continuously varying character.

The results show the mechanistic sensitivity and complexity of PCET reactions with water as proton acceptor and provide experimental model systems for several different PCET mechanisms. The intramolecular laser flash-quench reactions allow the CEP and PTET reactions of the TyrOH species to be distinguished from the very reactive TyrO$^-$ that dominates in bimolecular reactions. This allows us to distinguish the PTET of TyrOH (region C) from the ET of TyrO$^-$ (region D). The experimental pH-dependence of the CEP reaction (region B), with a rate that is proportional to $10^{0.5pH}$, is further established and now also observed in **Ru$_{dmb}$–Y** and **Ru$_{dmb}$–Y**. We report the surprising observation that this rate was rather insensitive to the difference in Ru$^{III/II}$ potential, from 1.10 to 1.53 V vs NHE, which is strong evidence against driving force variations as an explanation for the unusual pH-dependence in region B.[22,23] However, this result is also at odds with conventional expectations for both ETPT and CEP reactions, and the observed rates are too high to be consistent with simple PT-limited reactions. We furthermore note that this result is in contrast to the results of analogous tryptophan systems, where the CEP reaction did depend on the Ru$^{III/II}$ and TrpH$^{\bullet+}$/TrpH potentials.[45,49] The contrasting behavior for the tyrosine and tryptophan systems is not understood at this point, but our study provides further experimental basis for development of a microscopic model for the CEP reaction.

EXPERIMENTAL SECTION

Ru$_{dmb}$–Y and Ru$_{tmb}$–Y. These compounds were prepared in analogy with the synthesis of **Ru$_{bpy}$–Y** described in ref 37, and the details are listed in the Supporting Information. The experimental setup has been described elsewhere.[24] The samples were prepared using 20–50 μM of the Ru complexes, 10–150 mM of methyl viologen (Aldrich, 98%) or ca. 11–16 mM of $[Co(NH_3)_5Cl]Cl_2$ (Aldrich, 99.995%) dissolved in Milli-Q water (17 MΩ). As buffer either 0.5 mM Na_2HPO_4 (Sigma, 99%) or a 50:50 mixture of Na_2HPO_4 and H_3BO_3 (anhydrous powder, Sigma, 99.5%) at 0.5 or 2 mM was used. The use of different buffer concentrations did not give any significant difference of the observed rate constant at pHs where both buffer concentrations where used. Data in unbuffered solution showed more scatter due to a larger uncertainty in and instability of pH,[24] but the average values did not differ significantly from those obtained in 0.5 mM buffer. Samples were thermostated to 298 K and purged with Ar(g) for at least 10 min before and during the measurement. Isotope effects were measured using D_2O (Aldrich, 99.9% atom purity) as solvent assuming the exchange of the protons in buffer and compound is faster than sample preparation. The solution pH was measured in the optical cell, before and after the experiments, and did not change significantly. The release of NH_3 from the sacrificial acceptor $[Co(NH_3)_5Cl]^{2+}$ during experiments did not affect the pH. The p*D* was determined by subtracting 0.4 from the reading of a standard pH meter.[51]

At pH > 7 the PCET reaction was rapid enough that bimolecular recombination with the acceptor ($MV^{\bullet+}$) could be ignored. The rate constant was determined from the single exponential fit to the ΔAbs traces for Ru^{II} absorption at 450 nm and Y$^{\bullet}$ formation at 410 nm [Figures 3, 4, and S1 (Supporting Information)]. At pH < 7 the recombination reaction with $MV^{\bullet+}$ competed with PCET in the recovery of the Ru^{II}. The kinetic traces were then fitted using

$$[Ru^{II}] = [Ru^{II}]_0 e^{-kt}[MV^{\bullet+}]_0/(1 + k_{SO}[MV^{\bullet+}]_0 t) \quad (11)$$

where k is the rate constant for intramolecular PCET with Y, and k_{SO} is the second-order rate constant for the $MV^{\bullet+}$ decay as determined at 600 nm.[24] Experiments with the sacrificial acceptor $[Co(NH_3)_5Cl]^{2+}$ instead eliminated recombination and gave the same PCET rate constant as with MV^{2+}. On the basis of the transient absorption changes, ca. 1 μM of Ru^{III}–TyrOH was generated in each flash. This reacted quantitatively to give Ru^{II}–TyrO$^{\bullet}$ (eq 6) under conditions when recombination with $MV^{\bullet+}$ could be ignored. In experiments with the reversible acceptor MV^{2+}, both the Ru^{III} and TyrO$^{\bullet}$ species were reduced rapidly enough that they did not decompose or dimerize, so no changes of the kinetics were observed even after hundreds of laser flashes to the same sample. The integrity of the complex at the highest and lowest pH values employed was confirmed by readjusting the pH to neutral values and comparing the PCET kinetics and LC–MS analysis with that for a reference sample at neutral pH.

ASSOCIATED CONTENT

Supporting Information

Additional experimental details and data. This material is available free of charge via the Internet at http://pubs.acs.org.

AUTHOR INFORMATION

Corresponding Author

Leif.Hammarstrom@kemi.uu.se

Present Address

[‡]Visiting researcher from Northwestern University.

Author Contributions

[†]These authors contributed equally to the work.

Notes

The authors declare no competing financial interest.

■ ACKNOWLEDGMENTS

This work was supported by the Swedish Research Council, the Swedish Energy Agency, and the K&A Wallenberg Foundation. T.F.M. acknowledges the Wenner-Gren Foundation for a postdoc fellowship. A.M.S. acknowledges support from the Nanoscale Science and Engineering Initiative of the National Science Foundation under NSF Award Number EEC-0118025.

■ REFERENCES

(1) Dempsey, J. L.; Winkler, J. R.; Gray, H. B. *Chem. Rev.* **2010**, *110*, 7024−7039.
(2) Stubbe, J.; Nocera, D. G.; Yee, C. S.; Chang, M. C. Y. *Chem. Rev.* **2003**, *103*, 2167−2201.
(3) Aubert, C.; Vos, M. H.; Mathis, P.; Eker, A. P. M.; Brettel, K. *Nature* **2000**, *405*, 586−590.
(4) Dau, H.; Haumann, M. *Science* **2006**, *312*, 1471−1472.
(5) Renger, G. *Biochim. Biophys. Acta* **2004**, *1655*, 195−204.
(6) Okamura, M. Y.; Paddock, M. L.; Graige, M. S.; Feher, G. *Biochim. Biophys. Acta* **2000**, *1458*, 148−163.
(7) Faxen, K; Gilderson, G.; Adelroth, P.; Brezinski, P. *Nature* **2005**, *437*, 286−289.
(8) Belevich, I.; Verkhovsky, M. I.; Wikstrom, M. *Nature* **2006**, *440*, 829−832.
(9) Fontecilla-Camps, J. C.; Volbeda, A.; Cavazza, C.; Nicolet, Y. *Chem. Rev.* **2007**, *107*, 4273−4303.
(10) Lewis, N. S.; Nocera, D. G. *Proc. Natl. Acad. Sci. U. S. A.* **2006**, *103*, 15729−15735.
(11) Magnuson, A.; Anderlund, M.; Johansson, O; Lindblad, P; Lomoth, R; Polivka, T; Ott, S; Stensjo, K; Styring, S; Sundstrom, V; Hammarström, L. *Acc. Chem. Res.* **2009**, *42*, 1899−1909.
(12) Hambourger, M.; Moore, G.; Kramer, D.; Gust, D.; Moore, A. L.; Moore, T. A. *Chem. Soc. Rev.* **2009**, *38*, 25−35.
(13) Huynh, M. H. V.; Meyer, T. J. *Chem. Rev.* **2007**, *107*, 5004−5064.
(14) Mayer, J. M. *Annu. Rev. Phys. Chem.* **2004**, *55*, 363−390.
(15) Reece, S. Y.; Nocera, D. G. *Annu. Rev. Biochem.* **2009**, *78*, 673−699.
(16) Hammes-Schiffer, S.; Soudackov, A. V. *Chem. Rev.* **2010**, *110*, 6939−6960.
(17) Costentin, C. *Chem. Rev.* **2008**, *108*, 2145−2179.
(18) Warren, J. J.; Mayer, J. M. *Proc. Natl. Acad. Sci. U. S. A.* **2010**, *107*, 5282−5287.
(19) Styring, S.; Hammarström, L. *Energy Environ. Sci.* **2011**, *4*, 2379−2388.
(20) Yella, A.; Lee, H. W.; Tsao, H. N.; Yi, C.; Chandiran, A. K.; Nazeeruddin, M. K.; Diau, E. W-G.; Yeh, C.-Y.; Zakeeruddin, S. M.; Gratzel, M. *Science* **2011**, *334*, 629−634.
(21) Gunes, S.; Neugebauer, H.; Sariciftci, N. S. *Chem. Rev.* **2007**, *107*, 1324−1338.
(22) Sjödin, M.; Styring, S.; Åkermark, B.; Sun, L. C.; Hammarström, L. *J. Am. Chem. Soc.* **2000**, *122*, 3932−3936.
(23) Sjödin, M.; Styring, S.; Wolpher, H.; Xu, Y. H.; Sun, L. C.; Hammarström, L. *J. Am. Chem. Soc.* **2005**, *127*, 3855−3863.
(24) Irebo, T.; Reece, S. Y.; Sjödin, M.; Nocera, D. G.; Hammarström, L. *J. Am. Chem. Soc.* **2007**, *129*, 15462−15464.
(25) Costentin, C.; Louault, C.; Robert, M.; Saveant, J.-M. *Proc. Natl. Acad. Sci. U. S. A.* **2009**, *106*, 18143−18148.
(26) Costentin, C.; Robert, M.; Saveant, J. M. *J. Am. Chem. Soc.* **2007**, *129*, 5870−5879.
(27) Bonin, J.; Costentin, C.; Louault, C.; Robert, M.; Routier, M.; Saveant, J.-M. *Proc. Natl. Acad. Sci. U. S. A.* **2010**, *107*, 3367−3372.
(28) Bonin, J.; Costentin, C.; Louault, C.; Robert, M.; Saveant, J. M. *J. Am. Chem. Soc.* **2011**, *133*, 6668−6674.
(29) Costentin, C.; Louault, C.; Robert, M.; Saveant, J. M. *J. Am. Chem. Soc.* **2008**, *130*, 15817−15819.
(30) Fecenko, C. J.; Meyer, T. J.; Thorp, H. H. *J. Am. Chem. Soc.* **2006**, *128*, 11020−11021.
(31) Fecenko, C. J.; Thorp, H. H.; Meyer, T. J. *J. Am. Chem. Soc.* **2007**, *129*, 15098−15099.
(32) Song, N.; Stanbury, D. M. *Inorg. Chem.* **2008**, *47*, 11458−11460.
(33) Ishikita, H.; Soudackov, A. V.; Hammes-Schiffer, S. *J. Am. Chem. Soc.* **2007**, *129*, 11146−11152.
(34) Harriman, A. *J. Phys. Chem.* **1987**, *91*, 6102−6104.
(35) Lind, J.; Shen, X.; Eriksen, T. E.; Merenyi, G. *J. Am. Chem. Soc.* **1990**, *112*, 479−482.
(36) Krishtalik, L. I. *Biochim. Biophys. Acta* **2003**, *1064*, 13−21.
(37) Magnuson, A.; Berglund, H.; Korall, P.; Hammarström, L.; Åkermark, B.; Styring, S.; Sun, L. C. *J. Am. Chem. Soc.* **1997**, *119*, 10720−10725.
(38) Sjödin, M.; Irebo, T.; Utas, J. E.; Lind, J.; Merenyi, G.; Åkermark, B.; Hammarström, L. *J. Am. Chem. Soc.* **2006**, *128*, 13076−13083.
(39) Lytle, F. E.; Hercules, D. M. *Photochem. Photobiol.* **1971**, *13*, 123−133.
(40) Bimolecular reactions between Ru^{III} and TyrOH or $TyrO^-$ are much slower than the observed intramolecular reaction, as the total concentration of the Ru−TyrOH complexes is only ca. 3×10^{-5} M. The bimolecular rate constants for oxidation by $Ru^{III}(bpy)_3$ is ca. 1×10^6 and 3.5×10^9 M^{-1} s^{-1} for phenol and phenolate, respectively (ref 38). At pH = 10 the latter gives a pseudo-first-order rate constant of $<1 \times 10^4$ s^{-1}, which is already 2 orders of magnitude below the observed value for **Ru−Y**, and the tyrosinate fraction decreases rapidly at lower pH.
(41) Eigen, M. *Angew. Chem. Int. Ed. Engl.* **1964**, *3*, 1−19.
(42) With a $pK_a \approx 10$, deprotonation of tyrosine by H_2O is very slow (Scheme 1, left panel): $K_a = k_{PT1}/k_{-PT1}$, which with a diffusion controlled protonation by H_3O^+ ($k_{-PT1} \approx 1 \times 10^{11}$ M^{-1} s^{-1}) gives $k_{PT1} \approx 10$ s^{-1}. Instead, diffusion-controlled deprotonation by OH^- (right panel) will dominate at most pH values, for which k'_{PT1} should be on the order of 1×10^{10} M^{-1} s^{-1}; see ref 41. For the corresponding protonation by H_2O, and the relation $k'_{-PT1} = 10^{(pK_w - pK_a)}/k'_{PT1}$, we then obtain $k'_{-PT1} \approx 1 \times 10^6$ M^{-1} s^{-1}. This is much smaller than $k_{ET2} \geq 3 \times 10^7$ s^{-1}, as measured for Ru^{III}−$TyrO^-$ at high pH. Thus, the fraction of Ru^{III}−$TyrO^-$ created in each laser flash will react by ET much faster than it will be protonated. Also, if Ru^{III}−TyrOH reacts by PTET this will should be rate-limited by the initial PT step (k'_{PT1}).
(43) Bell, R. P. *The Proton in Chemistry*, 2nd ed.;Cornell University Press: New York, 1973.
(44) Gutman, M.; Nachliel, E. *Biochim. Biophys. Acta* **1995**, *1321*, 123−138.
(45) Zhang, M.-T.; Hammarström, L. *J. Am. Chem. Soc.* **2011**, *133*, 8806−8809.
(46) Irebo, T.; Johansson, O.; Hammarström, L. *J. Am. Chem. Soc.* **2008**, *130*, 9194−9195.
(47) Johannissen, L. O.; Irebo, T.; Sjödin, M.; Johansson, O.; Hammarström, L. *J. Phys. Chem. B* **2009**, *113*, 16214−16225.
(48) Marcus, R. A.; Sutin, N. *Biochim. Biophys. Acta* **1985**, *811*, 265−322.
(49) Zhang, M-T; Nilsson, J.; Hammarström, L. *Energy Environ. Sci.* **2012**, *5*, 7732−7736.
(50) See e.g. (a) Masuda, A.; Kaizu, Y. *Inorg. Chem.* **1998**, *37*, 3371. (b) Khundkar, L. R.; Perry, J. W.; Hanson, J. E.; Dervan, P. D. *J. Am. Chem. Soc.* **1994**, *116*, 9700. (c) McMahon, L. P.; Colucci, W. J.; McLaughlin, M. L.; Barkley, M. D. *J. Am. Chem. Soc.* **1992**, *114*, 8442−8448.
(51) Covington, A. K.; Paabo, M.; Robinson, R. A.; Bates, R. G. *Anal. Chem.* **1968**, *40*, 700−706.